Check for updates

Original Research Article

Mechanism of Cucurbitacin's Inhibition of Autophagy in Lung Cancer and Its Study in Magnetic Nano Piggyback System

Pharmacognosy Magazine
22(3) 1139–1149, 2026
© The Author(s) 2025
Article reuse guidelines:
in.sagepub.com/journals-permissions-india
DOI: 10.1177/09731296251371926
journals.sagepub.com/home/phm
Sage

Zhifei Zhao[1], Meng Yu[1], Wenfu Shi[1] and Tao Zhang[2]

Abstract

Background: The mortality rate of lung cancer is increasing. Ferric oxide nanoparticles are magnetic and biocompatible nanomedicines. Cucurbitacin has anti-tumor activity. Its pharmacological effects and molecular mechanisms have attracted widespread attention. Research shows that cucurbitacin has good anti-cancer activity. Research on the molecular mechanism of ferric oxide nanoparticles carrying cucurbitacin inhibiting the development of lung cancer through Beclin-1 (BECN1) regulation of autophagy was carried out in the context of the many challenges faced by the current treatment of lung cancer.
Objectives: This study intends to investigated the mechanism of cucurbitacin's inhibition of autophagy in lung cancer.
Materials and Methods: A549 cells were assigned to the negative control (NC) group, Fe_3O_4–Cu group, cucurbitacin (Cu) group, BECN1-inhibitor group, and BECN1-mimics group. The normal lung cell line, BEAS-2B, was taken as a control group. Fe_3O_4–Cu nanomaterials were prepared and used in cell experiments to observe the biological activity of A549 cells and the expression of BECN1-related genes.
Results: Fe_3O_4–Cu was successfully prepared and found to have a good tumor suppressor effect in lung cancer. BECN1-inhibitor and BECN1-mimics were used to intervene in A549 cells, respectively. We found that promoting BECN1 expression is beneficial for promoting the autogenesis of A549 cells. In the process of upregulating the expression of BECN1, Fe_3O_4–Cu affects the autophagy-related proteins ATG5 and p62, thereby promoting autophagy and inhibiting the activities of lung cancer cells to a certain extent.
Conclusion: BECN1 is involved in lung cancer. Fe_3O_4–Cu can actively inhibit the proliferation and migration of lung cancer cells and promote cell apoptosis. This is achieved by regulating the expression of BECN1. Fe_3O_4–Cu can promote BECN1 expression and affect the production of autophagy-related proteins, thereby promoting Lung cancer cell autophagy, thereby inhibiting the development of lung cancer, which provides a new nanomedicine delivery strategy for the treatment of lung cancer.

Keywords

Ferric oxide, nanoparticles, cucurbitacin, Beclin-1, autophagy, lung cancer

Received 18 December 2024; **revised** 15 May 2025; **accepted** 29 July 2025

Introduction

Lung cancer involves multiple factors and pathways. Although several chemotherapeutic drugs are available, the overall survival rate of lung cancer patients is still low (Nooreldeen & Bach, 2021; Zanders et al., 2022). Studies have shown (Zhou, Cui et al., 2021; Zhou, Wang et al., 2021) that high expression of autophagy-related genes such as ATG5, ATG7, and LC3 is associated with lung cancer risk. In addition, the K-Ras oncogene and TP53 tumor suppressor gene are also related to the regulation of autophagy and are involved in the occurrence of lung cancer (Yuan et al., 2022). These provide a certain basis for the exploration of the mechanism of autophagy in lung cancer.

Modern pharmacological research shows that cucurbitacin has various biological activities, such as anti-tumor, hepatoprotective, anti-inflammatory, and improving immunity (Yuan et al., 2021). Cucurbitacin E can effectively inhibit the activity of the Janus Kinase 2/signal transducer and activator of transcription 3 (JAK2/STAT3) signaling pathway. CuE interacts with JAK2, preventing the phosphorylation of the kinase domain of JAK2 and STAT3,

[1]Department of Oncology, Beichen District Traditional Chinese Medicine Hospital Affiliated to Tianjin University of Traditional Chinese Medicine, Tianjin, China

[2]Department of Orthopaedics, Beichen District Traditional Chinese Medicine Hospital Affiliated to Tianjin University of Traditional Chinese Medicine, Tianjin, China

Corresponding author:
Tao Zhang, Department of Orthopaedics, Beichen District Traditional Chinese Medicine Hospital Affiliated to Tianjin University of Traditional Chinese Medicine, No. 436 Beijing Tianjin Highway, Tianjin 300400, China.
E-mail: yijizhui05866@126.com

Creative Commons Non Commercial CC BY-NC: This article is distributed under the terms of the Creative Commons Attribution-NonCommercial 4.0 License (http://www.creativecommons.org/licenses/by-nc/4.0/) which permits non-Commercial use, reproduction and distribution of the work without further permission provided the original work is attributed as specified on the SAGE and Open Access pages (https://us.sagepub.com/en-us/nam/open-access-at-sage).

resulting in the inability of STAT3 to transfer to the nucleus and bind to deoxyribonucleic acid (DNA), thereby inhibiting its-mediated gene expression (Ouyang et al., 2022; Zanders et al., 2022). In addition, cucurbitacin E can activate the cleavage of caspase-3 and PARP, leading to DNA fragmentation and thus inducing cell apoptosis. Studies have pointed out that CuE can also inhibit the transcription and translation of vascular endothelial growth factor (VEGF) by inhibiting key molecules such as mitogen-activated protein kinase (MAPK) and phosphoinositide 3-kinase (PI3K) in the signal transduction pathway, thereby exerting anti-cancer effects (Zhang et al., 2022). These demonstrate the substance's potential for research in lung cancer. Meanwhile, studies have shown that Beclin-1 (BECN1) regulates the cystine/glutamic acid reverse transport system by forming a complex with SLC7A11 and affects the autophagy sensitivity of lung cancer cells (Kim, Kim et al., 2022; Kim, Min et al., 2022). This complex induces apoptosis by activating specific enzyme systems and Bcl-2 family proteins, thereby exerting an inhibitory effect on the growth of lung cancer. However, can cucurbitacin affect the development of lung cancer by regulating the expression of BECN1? This still awaits further exploration.

Cucurbitacin E has received widespread attention in the field of nanotechnology. Its special properties and potential application value make it a highly respected nanomaterial (Zheng et al., 2022). Studies have shown that cucurbitacin has excellent photothermal conversion effects and fluorescence properties and can be used as a photothermal therapy and fluorescence imaging reagent in tumor treatment and cell imaging research. At the same time, it can also be used as a glucose-sensitive material or a virus sensor (Yang et al., 2020). At the nanoscale, its excellent biocompatibility, biological activity, antioxidant, and anti-bacterial properties have further promoted the application of this compound in fields such as drug delivery, bioimaging, sensors, and photoelectrocatalysis (Lin & Farooqi, 2021). Ferric tetroxide nanoparticles can be used as drug carriers to accurately deliver drugs to the lesion through magnetic field guidance to improve the therapeutic effect of the drug and reduce side effects (Basha et al., 2021; Brouwer et al., 2020). Combined with the biological activity of cucurbitacin E, it can further enhance the effectiveness of drug delivery, efficiency, and therapeutic effect (Brouwer et al., 2020). Therefore, it will be of great significance to use ferric oxide nanoparticles to carry cucurbitacin to treat diseases. In this study, we prepared Fe_3O_4 nanoparticles and combined them with bioactive drugs such as cucurbitacin E to develop new nanomedicines, provide new strategies and targets for lung cancer treatment, and deepen the regulation mechanism of BECN1 and autophagy.

Materials and Methods

Experimental Materials

Human lung adenocarcinoma A549 cells (Wuhan Shangen Biotechnology); normal lung cell line, BEAS-2B (Suzhou Haixing Biotechnology).

Cucurbitacin (Cu, purity: ≥98.0%, batch number: 7257-29-6, Shandong East Asia Chemical); BECN1-inhibitor, BECN1-mimics (Shenzhen Zhenqiang Biotechnology); ATG5 monoclonal antibody (Shanghai Shengke Biotechnology); p62 monoclonal antibody (Shanghai Bowan Biotech); secondary antibody (Shanghai Uniview Biotech).

The chemical structural formula of the relevant materials is shown in Figure 1.

Preparation of Fe_3O_4–Cu Nanomaterials

Weigh 10.9 g $FeSO_4 \cdot 7H_2O$ and 4.0 g $FeCl_3 \cdot 6H_2O$ and dissolve them in 30 mL deionized water. Pour in nitrogen and add 2 mL of hydrazine hydrate while stirring with a mechanical stirrer. Then, add 35 mL of concentrated ammonia dropwise to adjust the pH of the solution to 9. After stirring for 30 min, the system was heated to 80°C and aged for 1 h. The reaction was stopped, and a magnet was used for magnetic separation to collect the lower solids, which were washed with deionized water, then with absolute ethanol, and finally dried at 60°C for 12 h to obtain Fe_3O_4 nanoparticles.

Preparation of Fe_3O_4–Cu Nanoparticles

Weigh 4 mg Fe_3O_4 and dissolve it in 4 mL of 1% acetic acid solution. After all, Fe_3O_4 is dissolved, adjust the pH value to 5 with 2 mol/L NaOH solution. Weigh 0.25, 0.5, 0.75, and 1 mg of Cu and dissolve them in 500 μL of anhydrous methanol. Then, add them dro pwise to the Fe_3O_4 solution (20 drops/min). After the dropwise addition is completed, an equal volume of 1 mg/mL tripolyphosphate (TPP) solution is added dropwise, and the cross-linking reaction is stirred for 30 min to prepare Fe_3O_4–Cu nanoparticles. Filter and store at 4°C.

Fe_3O_4–Cu morphology was observed by transmission electron microscope, and its zeta potential was measured.

Experimental Methods

Cell Culture, Grouping and Transfection

All cells were cultured in Roswell Park Memorial Institute-1640 (RPMI-1640) medium and digested and passaged when the cell confluence reached 80%. A549 cells were assigned to a negative control group (NC group),

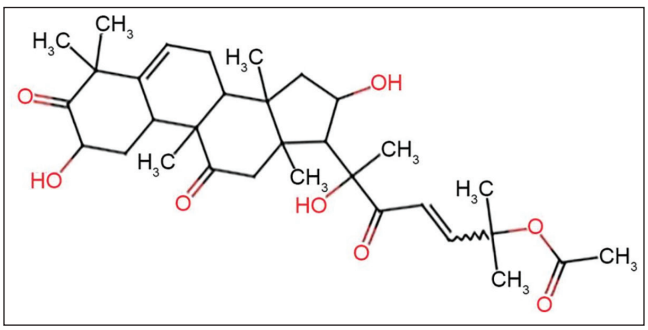


Figure 1. Molecular Structural Formula of Cucurbitacin.

Fe_3O_4–Cu group (transfected with Fe_3O_4–Cu nanoparticles), Cu group (transfected with Cu), BECN1-inhibitor group (transfected with BECN1-inhibitor), and BECN1-mimics group (transfected with BECN1-mimics).

At the same time, BEAS-2B was selected as the control group, without any nanoparticles or drugs. The Fe_3O_4–Cu group transfected 0.75 mg of Cu to prepare Fe_3O_4–Cu; In the Cu group, 0.75 mg of Cu was transfected without nanoparticles. The BECN1-inhibitor group was transfected with small interfering RNA (siRNA) (sequence: 5′-GCAUUCAGA UGAUCGGAUA-3′) at 50 nM and Lipofectamine 3000 for 24 h. The BECN1-mimics group used the BECN1 plasmid (vector pEX-2, concentration 1 μg/mL) and transfected for 48 h.

After the cells continued to be cultured for 24 h, subsequent experimental operations were performed.

Cell Proliferation

Cells were seeded and cultured in a humidified incubator for 12 h. Then discard the culture medium, add 10 μL 3-(4,5-dimethylthiazol-2-yl)-2,5-diphenyltetrazolium bromide (MTT) solution and 100 μL fresh Dulbecco's modified Eagle medium (DMEM), and continue culturing for 4 h. Place it on the floor with low-speed shaking for 10 min to dissolve fully. A microplate reader measures the absorbance. Calculate the cell survival rate (%) = average absorbance value of the experimental group/average absorbance value of the control group × 100%.

Cell Migration

After digestion, the A549 cells in the logarithmic growth phase were inoculated into a culture plate containing six wells. After adjusting the cell density, they were cultured for 24 h. When the cell confluence rate exceeds 90%, the migration ability is observed by the scratch experiment.

Apoptosis

After digestion, they were made into a suspension of 1×10^6 mL. After centrifugation and washing with PBS, 150 μL of suspension was mixed with 10 μL of buffer, 5 μL of Annexin V-FITC dye, and 5 μL of PI dye for 15 min. After the incubation was completed, the mixture was observed using a flow cytometer.

Autophagy

A549 cells were seeded in a laser confocal culture dish, and 5 μL of Lipofection™ 3000 transfection reagent was mixed with 500 ng of EGFP-LC3 plasmid in a six-well plate, cultured at room temperature for 6 h, the culture medium was replaced, and an inverted confocal was used after culturing again for 24 h. The autophagy of tumor cells was observed under a microscope, and the number of EGFP-LC3 in A549 cells was counted.

Reverse Transcription Polymerase Chain Reaction (RT-PCR)

Logarithmically growing cells were harvested, reverse transcribed, and analyzed by RT-PCR. All messenger ribonucleic acid (mRNA) expression values are presented relative to glyceraldehyde-3-phosphate dehydrogenase (GAPDH), and relative levels were estimated using the $2^{-\Delta\Delta Ct}$ method. Table 1 lists the primers and primer sequences.

Western Blotting

Logarithmically grown cells were harvested, digested, and the protein concentration was detected. Separate, transfer (10% sodium dodecyl sulfate–polyacrylamide gel electrophoresis (SDS-PAGE)), and incubate with primary antibody. Wash and incubate the membrane with HRP-labeled secondary antibody for 1 h. Detection was enhanced by the internal reference GAPDH.

Statistical Analysis

All the data were processed and analyzed by GraphPad Prism 8.0.2. Data were expressed as mean ± standard deviation. The Shapiro–Wilk test was used for normality tests ($p > .05$ was regarded as a normal distribution). In the intergroup comparison, normal data were tested using univariate analysis of variance (ANOVA) (F-test for homogeneity of variance passed), and non-normal data were tested using the Kruskal–Wallis test. *Post hoc* multiple comparisons were conducted using the Tukey method, with $p < .05$ being the significance threshold. All experiments were repeated in three independent biological replicates, each containing six technical replicates.

Table 1. Real-time Polymerase Chain Reaction (PCR) Primers and Primer Sequences.

Primers		Sequences
BECN1	Forward primer	5′-TATCGCTCAGAAGGAGATCA-3′
	Reverse primer	5′-GCTGCTCCCAGTTTTCAGTT-3′
GAPDH	Forward primer	5′-AAAGGGTCATCATCTCCGCC-3′
	Reverse primer	5′-AGTGATGGCATGGACTGTGG-3′

Note: BECN1: Beclin-1; GAPDH: Glyceraldehyde-3-phosphate dehydrogenase.

Results

Fe_3O_4–Cu Nanoparticles Were Successfully Prepared

In the transmission electron microscope image, Fe_3O_4–Cu appears as black or gray spherical particles with an average particle size of (12.35 ± 2.16) nm and is well dispersed (Figure 2A). The zeta potential of Fe_3O_4–Cu is −22.13 mV, indicating that the particles are stable (Figure 2B).

Effect of Fe_3O_4–Cu on Lung Cancer Cell Inhibition Rate

Compared with the 0.25 mg group, the number of A549 cell clones in the 0.5, 0.75, and 1 mg Fe_3O_4–Cu groups decreased significantly ($p < .05$) in a concentration-dependent manner. Meanwhile, when the dose was 0.75 mg, the inhibition rate of Fe_3O_4–Cu on the viability of A549 cells reached 70%, and its toxicity to normal BEAS-2B cells was less than 20%, as shown in Table 2. Therefore, in the subsequent experiments, 0.75 mg was set as the optimal dose of Cu in Fe_3O_4–Cu.

Fe_3O_4–Cu Has a Good Anti-cancer Effect in Lung Cancer

To explore the biological role of Fe_3O_4–Cu in lung cancer, after culturing the cells, we found that with the extension of time, the proliferation ability of lung cancer cells intervened by Fe_3O_4–Cu was only (113.84 ± 2.14)%, showing a significant proliferation inhibition phenomenon compared with the other two groups ($p < .05$, Figure 3A). Meanwhile, the proportion of cell migration in the Fe_3O_4–Cu group was (53.22 ± 4.65)%, indicating that the migration ability of the cells was significantly weakened (vs. other groups, $p < .05$, Figure 3B). Cell apoptosis in the Fe_3O_4–Cu group also confirmed this phenomenon (vs. other groups, $p < .05$, Figure 3C). During this period, we found that Cu has a positive inhibitory effect on lung cancer, with Fe_3O_4–Cu being the most prominent.

BECN1 Expression is Reduced in Lung Cancer and Promoting its Expression Can Induce Autophagy in Lung Cancer Cells

BECN1 expression in A549 cells was significantly reduced (vs. the control group, $p < .05$, Figure 4A,B). In order to explore the impact of BECN1 on lung cancer activity, we first used BECN1 inhibitor and BECN1 mimics to intervene in A549 cells, respectively, and found that BECN1 was significantly reduced in cells treated with BECN1 inhibitor. In contrast, in the BECN1 mimics group, the expression of BECN1 levels in cells showed an opposite trend (vs. other groups, $p < .05$, Figure 4A,B), demonstrating the successful intervention of BECN1-inhibitor and BECN1-mimics on BECN. When further observing A549 cells, it was found that BECN1-mimics could induce autophagy in A549 cells, and the number of LC3

Table 2. Effects of Fe_3O_4–Cu on the Inhibition Rate of A549 Cells and the Cytotoxicity of BEAS-2B Cells.

Groups	*n*	A549 Cell Inhibition Rate (%)	BEAS-2B Cell Cytotoxicity (%)
0.25 mg	5	15.25 ± 2.33	9.36 ± 1.22
0.5 mg	5	50.65 ± 4.65*	13.33 ± 2.19*
0.75 mg	5	72.11 ± 5.59*	17.36 ± 2.71*
1 mg	5	84.36 ± 6.17*	23.98 ± 3.21*

Note: Compared with the 0.25 mg group, *$p < .05$.

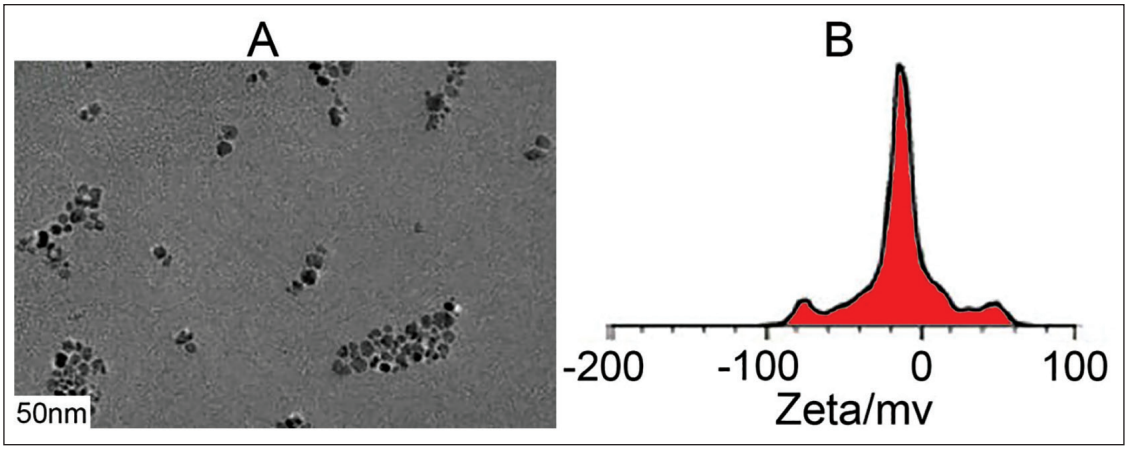


Figure 2. Transmission Electron Microscope Image of Fe_3O_4–Cu.

Note: (A) Transmission electron microscope image of Fe_3O_4–Cu, 50 nm; (B) potential distribution of Fe_3O_4–Cu nanoparticles.

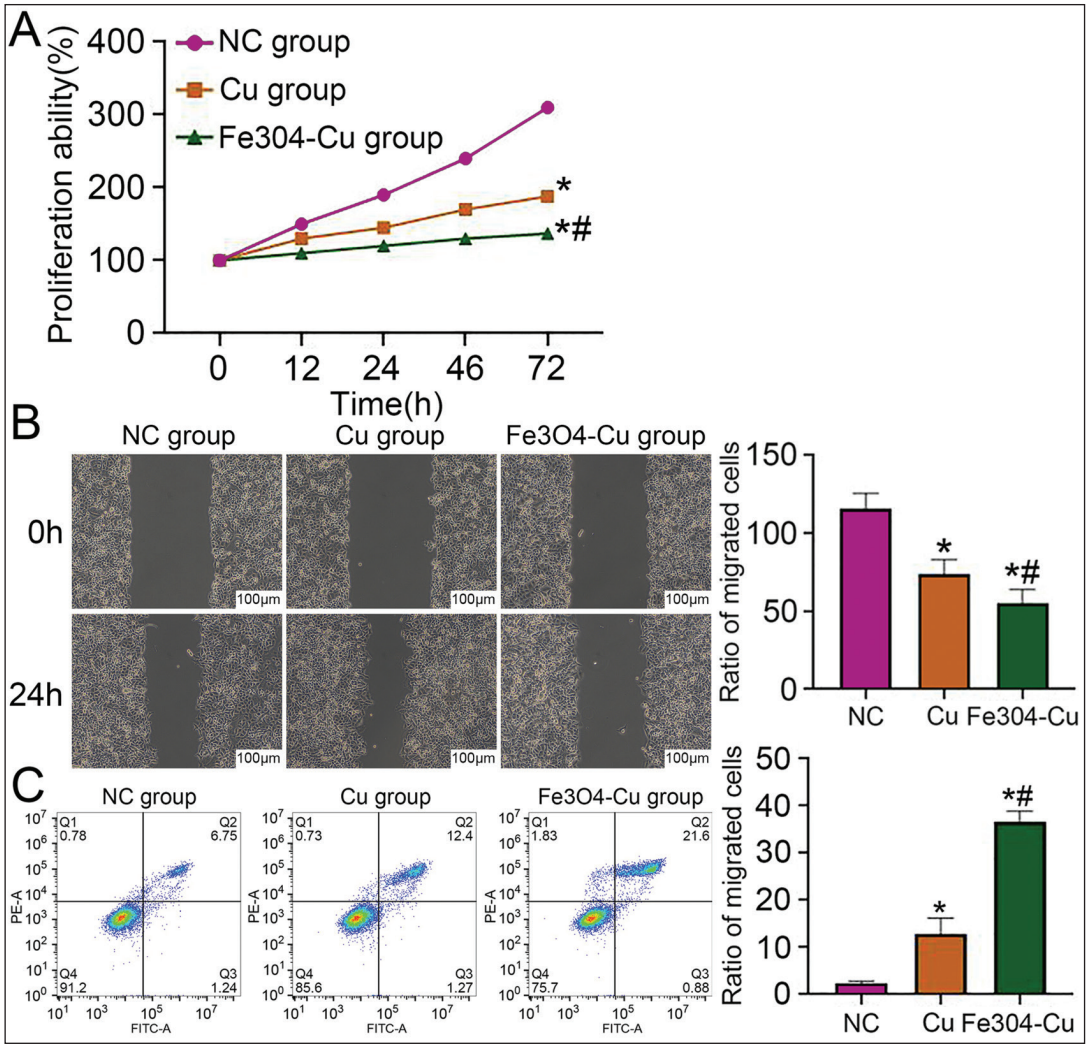


Figure 3. Fe_3O_4–Cu Has a Good Anti-tumor Effect in Lung Cancer (n = 6).

Notes: (A) 3-(4,5-Dimethylthiazol-2-yl)-2,5-diphenyltetrazolium bromide (MTT) experiment to detect the proliferation ability of A549 cells; (B) scratch test to observe the migration of A549 cells, and the histogram shows the migration ability; (C) flow cytometry to observe the apoptosis of A549 cells, and the histogram shows the apoptosis ability. Compared with negative control (NC) group, *p < .05; compared with Cu group, #p < .05.

puncta in the cells increased to (17.96 ± 1.32) (vs. other groups, p < .05, Figure 4C). Meanwhile, further experimental observations revealed that after adding BECN1-mimics to A549 cells, the expression of autophagy-related protein ATG5 significantly increased to 0.59 ± 0.03, while the expression of p62 decreased to 0.25 ± 0.06 (vs. other groups, p < .05, Figure 4D). The above experiments reflect that promoting BECN1 expression is beneficial for promoting autophagy in A549 cells. Furthermore, in further observations, it can be found that the protein expressions of PI3K, AKT, and mammalian target of rapamycin (mTOR) in the BECN1-mimics group were significantly decreased (Figure 4E), indicating that the expression of BECN1 can reduce the activity of the PI3K/AKT/mTOR signaling pathway.

Fe_3O_4–Cu Can Promote Autophagy in Lung Cancer Cells by Promoting BECN1 Expression, Thereby Affecting Lung Cancer Development

We observed a significant increase in BECN1 expression in Fe_3O_4–Cu (vs. NC group, p < .05, Figure 5A,B). To verify this, we added BECN1-mimic based on Fe_3O_4–Cu intervention and found that the proliferation and migration abilities of A549 cells were the weakest in the Fe_3O_4–Cu+BECN1-mimics group (vs. other groups, p < .05, Figure 5C,D), and at the same time, the apoptosis ability increased significantly (vs. other groups, p < .05, Figure 5E). At the same time, we added BECN1 inhibitor, which is opposite to BECN1 mimic, in the Fe_3O_4–Cu group. The proliferation, migration, and

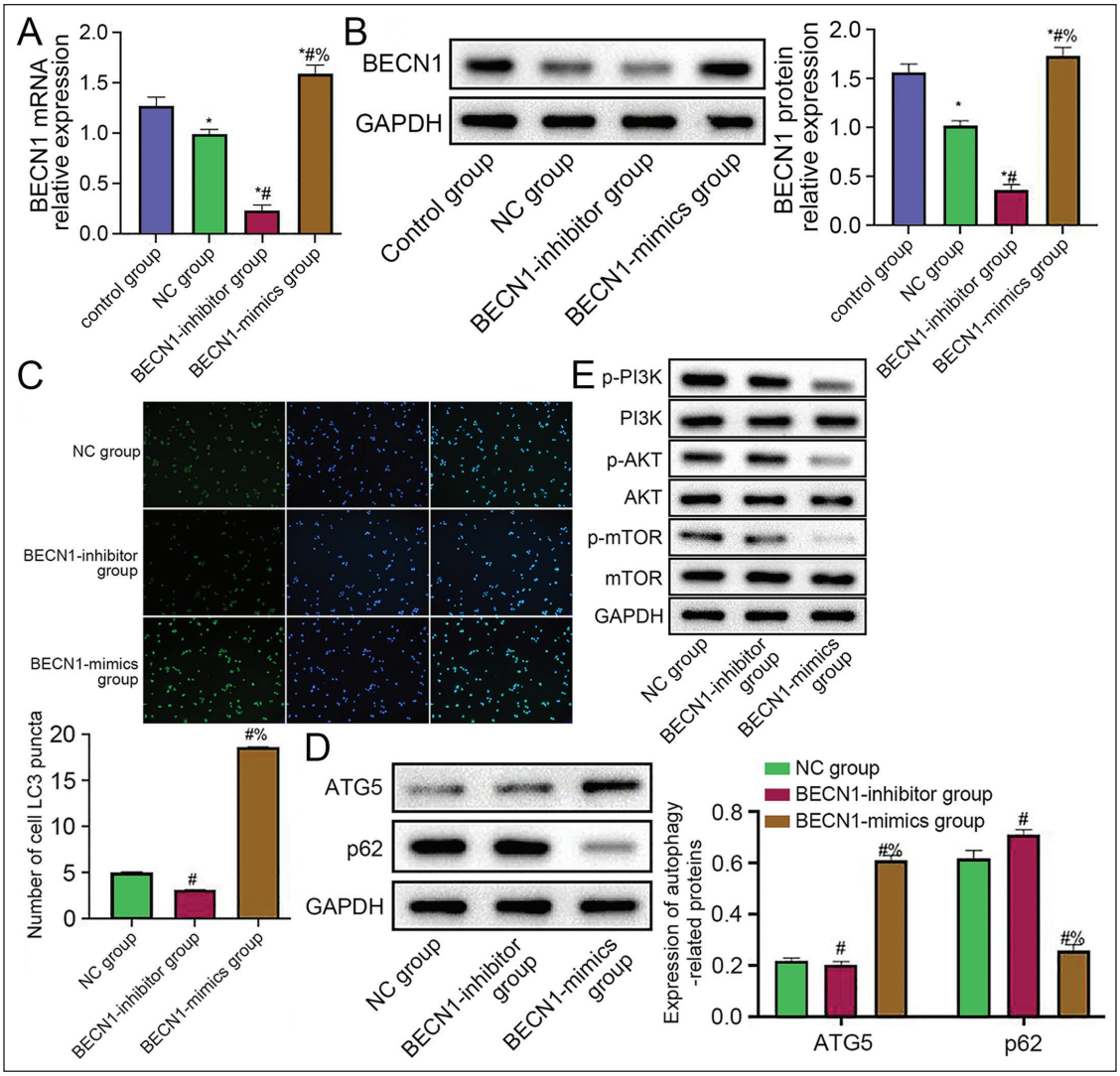


Figure 4. The Expression of Beclin-1 (BECN1) is Reduced in Lung Cancer, and Promoting Its Expression Can Induce Autophagy in Lung Cancer Cells (n = 6).

Notes: (A) Reverse transcription polymerase chain reaction (RT-PCR) to detect the relative expression of BECN1 messenger ribonucleic acid (mRNA); (B) Western blot (WB) experiment to detect the relative expression of BECN1 protein; (C) observation of autophagy under laser confocal microscope, 20 μm, histogram showing the expression of BECN1 protein in A549 cells number of LC3 puncta; (D) WB experiment to detect the relative expression of autophagy-related proteins; (E) WB experiment to detect the relative expression of phosphoinositide 3-kinase/protein kinase B (PI3K/AKT) pathway-related protein. Compared with the control group, *p < .05; compared with the negative control (NC) group, #p < .05; compared with the BECN1-inhibitor group, % p < .05.

apoptosis abilities of A549 cells were effectively reversed (vs. Fe_3O_4–Cu+BECN1 mimics group, $p < .05$, Figure 5C–5E). This also further verified that Fe_3O_4–Cu can promote BECN1 expression and inhibit A549 cells.

At the same time, further observation showed that the autophagy ability and LC3 puncta number of A549 cells in Fe_3O_4–Cu+BECN1-mimics group were significantly increased (vs. other groups, $p < .05$, Figure 5F), and ATG5 protein expression was increased, while p62 expression decreased significantly (vs. other groups, $p < .05$, Figure 5G), indicating that Fe_3O_4–Cu affects the autophagy-related proteins ATG5 and p62 in the process of upregulating BECN1 expression, thereby promoting autophagy in cells and inhibit the biological activity of lung cancer cells to a certain extent.

Discussion

Studies have found that cucurbitacin can interfere with the transcription process of the VEGF gene by affecting the activity of transcription factors or DNA-binding proteins, thereby reducing the production of VEGF and inhibiting angiogenesis (Torres-Moreno et al., 2020; Üremiş et al., 2022). Cucurbitacin can form dimers with the subunits p85

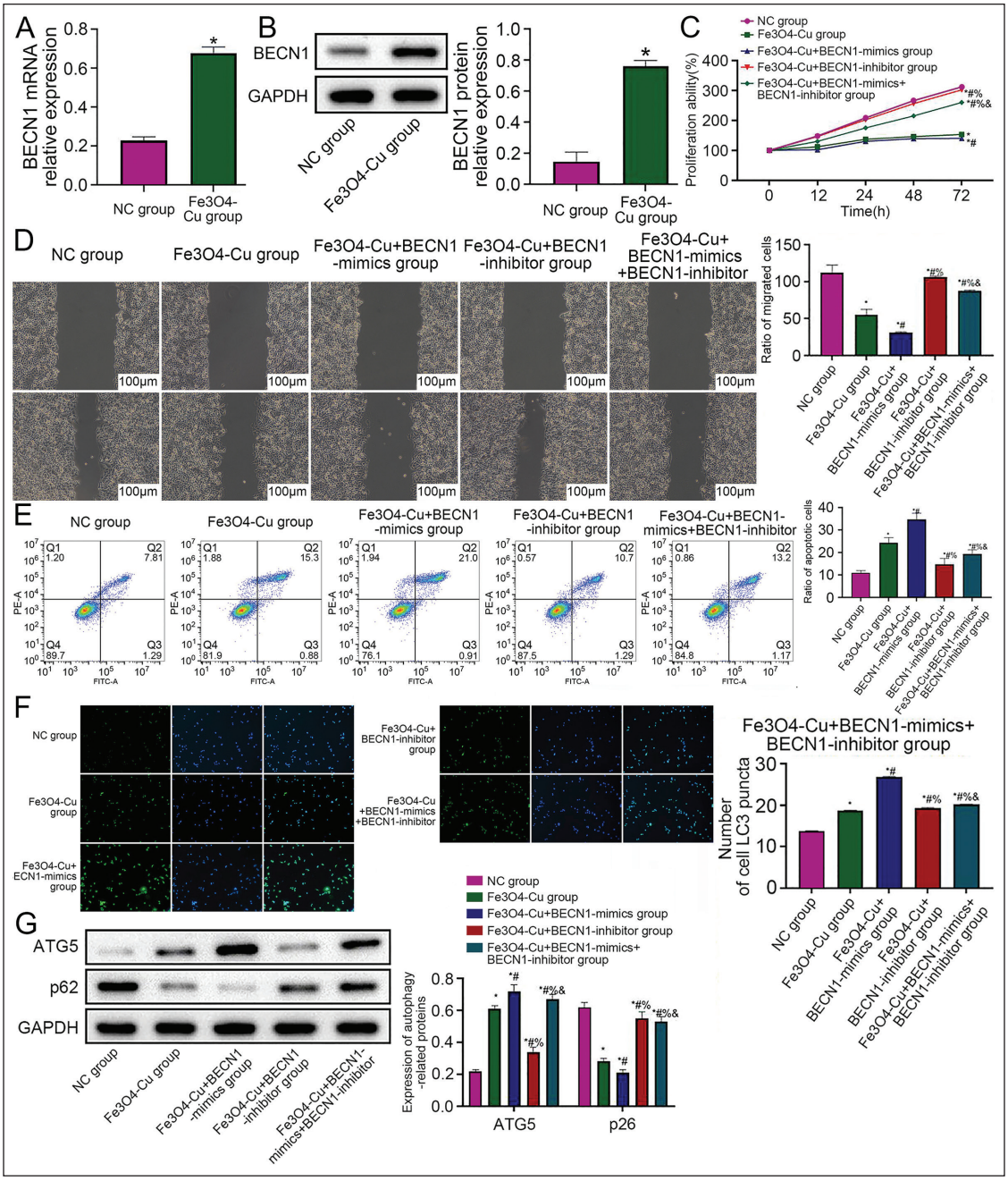


Figure 5. Fe_3O_4–Cu Can Promote Lung Cancer Cell Autophagy by Promoting Beclin-1 (BECN1) Expression, Thereby Affecting the Development of Lung Cancer (n = 6).

Notes: (A) Reverse transcription polymerase chain reaction (RT-PCR) to detect the relative expression of BECN1 messenger ribonucleic acid (mRNA); (B) WB experiment to detect the relative expression of BECN1 protein; (C) 3-(4,5-dimethylthiazol-2-yl)-2,5-diphenyltetrazolium bromide (MTT) experiment to detect the proliferation ability of A549 cells; (D) scratch test to observe the migration of A549 cells and the histogram shows the migration ability; (E) flow cytometry observation of A549 cell apoptosis, the histogram shows the apoptosis ability; (F) laser confocal microscopy observation of cell autophagy, 20 μm, the histogram shows that in A549 cells, the number of LC3 puncta; (G) Western blot (WB) experiment to detect the relative expression of autophagy-related proteins. Compared with negative control (NC) group, *p < .05; compared with Fe_3O_4–Cu group, #p < .05; compared with Fe_3O_4–Cu + BECN1-mimics group, % p < .05; compared with Fe_3O_4–Cu + BECN1-inhibitor group, & p < .05.

and p110 of PI3K and further prevent the binding of PI3K to growth factor receptors, inhibit PI3K to a certain extent, and further inhibit the tuberin phosphatase originally activated by Akt and the activity of mTOR, thus blocking cell proliferation (Deleyto-Seldas & Efeyan, 2021). In addition, cucurbitacin inhibits β-catenin nuclear translocation and can also inhibit c-Myc, cyclin D1, and so on, to a certain extent, thereby inhibiting tumor cells (He & Tang, 2020; Liu et al.,

2022). However, cucurbitacin has certain biochemical instability and is easily affected by environmental factors such as light, temperature, acid, and alkali, and its solubility is low under physiological conditions. Therefore, in order to improve the shortcomings of cucurbitacin, we used Fe_3O_4 to modify and transport it. Previous studies have shown that the surface of Fe_3O_4 nanoparticles carries a positive charge under acidic conditions, while TPP, as a polyanionic compound ($PO4^{3-}$), combines with Fe_3O_4 through electrostatic attraction to form a stable ionic cross-linking network (Wu et al., 2023). The porous structure formed after the cross-linking of TPP and Fe_3O_4 encapsulates hydrophobic Cu through hydrophobic interactions and hydrogen bonds, thereby significantly increasing the drug loading capacity of nanomaterials (Chandra et al., 2023). Meanwhile, the TPP cross-linking layer can shield the contact between Cu and hydrolases in body fluids, thereby better protecting the drug activity (Leng et al., 2022). The introduction of TPP not only improves the stability of nanoparticles through electrostatic cross-linking, but also the pH-responsive network formed by it realizes intelligent drug release in the tumor microenvironment. This design overcomes the defects of poor water solubility and easy degradation of cucurbitacin. It also lays the foundation for subsequent *in vivo* applications. Therefore, in the process of preparing nanomaterials in this study, addition of the TPP solution is regarded as a key technical link. In order to clarify the role of Fe_3O_4–Cu in lung cancer, we first found through cell culture experiments that with the intervention of cucurbitacin, cancer cell activities were significantly weakened. Fe_3O_4–Cu has a more consistent effect. This shows that Fe_3O_4–Cu has a good anti-tumor effect in lung cancer.

Studies have shown that BECN1 inhibits Janus kinase phosphorylation by interacting with gp130, thereby inhibiting STAT3 phosphorylation and nuclear translocation, ultimately inhibiting IL-6-induced cell proliferation and survival (Li et al., 2020). In addition, BECN1 can promote the release of Ca^{2+} from the endoplasmic reticulum into the cytoplasm, thereby inhibiting IL-6-induced Ca^{2+} influx and Ca^{2+}-dependent signal transduction pathways (Hirata et al., 2022; Liao et al., 2021). The inhibition of IL-6 further reduces the activation of STAT3, thereby reducing the responsiveness of tumor cells to IL-6 and inhibiting the growth and invasion ability of cancer cells. BECN1 expression can reduce the expression of GRP78 and the transmission of endoplasmic reticulum stress signals downstream of IRE1, PERK, ATF6, and other pathways, thereby affecting the stress response and viability of tumor cells (Ikeda et al., 2022; Sun et al., 2021). Furthermore, studies have shown that BECN1 clears damaged mitochondria by maintaining autophagic homeostasis (Guo et al., 2020), thereby preventing DNA mutations caused by ROS accumulation and further regulating the progression of pulmonary fibrosis (Kumari, Singh, Singh, 2024; Singh et al., 2025). Meanwhile, during the process of pulmonary fibrosis, the oxidative stress response of the body can further aggravate the recruitment of inflammatory cells in the lungs, accompanied by abnormal collagen repair, thereby promoting the growth of granulomatous nodules, which in turn leads to damaged mitochondrial deposition, thereby weakening the autophagy ability of mitochondria and aggravating pathological lesions (Kumari, Singh, Dash et al., 2024). We found significantly reduced BECN1 expression in A549 cells, and we speculated that it is related to the development of lung cancer. Therefore, we used BECN1-inhibitor and BECN1-mimics to intervene in A549 cells, respectively, and found that BECN1-mimics induced autophagy in A549 and increased the number of LC3 puncta in cells, suggesting that upregulating the expression of BECN1 can promote the growth of A549 cells. Autophagic process. At the same time, further experimental observations found that after adding BECN1-mimics to A549 cells, the expression of the autophagy-related protein ATG5 increased significantly, suggesting that it is related to lung cancer development, while p62 expression decreased, indicating that the expression of BECN1 was promoted. It is beneficial to promote autophagy in A549 cells. It was demonstrated that promoting the expression of BECN1 is beneficial to promoting autophagy in A549 cells and hints at the possible impact of BECN1 on the development of lung cancer. Previous studies have shown that the PI3K/AKT/mTOR pathway plays an important regulatory role in autophagy. Growth factor factors activate the PI3K/Akt/mTOR signaling axis. Activated and phosphorylated Akt can inhibit TSC1/2 and activate downstream mTOR1 (Dunn et al., 2022).

During this process, the activated mTORC1 interferes with the formation of the UNC-51-like autophagy-activated kinase complex, and autophagic activities are subsequently hindered (Chen et al., 2020). In this study, it can be found that the protein expression of the PI3K/Akt/mTOR pathway was downregulated in the BECN1-mimics group. The possible analysis of the reason is that the expression of BECN1 is upregulated, which promotes the transformation of LC3-II by antagonizing the release of autophagy initiating complex from Bcl-2. During this process, the PI3K-III complex is destroyed (Son et al., 2021; Zhang et al., 2020), thereby inhibiting the phosphorylation of AKT and blocking mTORC1. This further indicates that the promoting effect of BECN1 on autophagy in A549 cells may be achieved by inhibiting the expression of the PI3K/Akt/mTOR pathway. However, the specific mechanism of action still needs to be further explored. Through experiments, we observed that Fe_3O_4–Cu can increase the expression of BECN1. In order to clarify BECN1's role in lung cancer affected by Fe_3O_4–Cu, we added BECN1-mimic based on Fe_3O_4–Cu intervention and found that the apoptosis rate of A549 increased, and the autophagy capacity and LC3 puncta number of A549 cells increased significantly.

ATG5 protein expression increased significantly, and p62 expression decreased significantly, indicating the key role of BECN1 in the development of lung cancer affected by Fe_3O_4–Cu. Fe_3O_4–Cu+BECN1-inhibitor significantly reversed this

result, which not only shows that Fe_3O_4–Cu can promote lung cancer cell autophagy by promoting the expression of BECN1, thereby affecting the development of lung cancer, but also further supports the core role of BECN1 in Fe_3O_4–Cu treatment of lung cancer.

Conclusion

In summary, BECN1 is involved in lung cancer pathogenesis. Upregulating BECN1 expression in lung cancer cells can promote autophagy, and to a certain extent, it inhibits the activity of the PI3K/AKT/mTOR signaling pathway. In addition, we also found that Fe_3O_4–Cu can inhibit the behaviors of lung cancer cells and promote apoptosis by regulating BECN1 expression. These findings provide important clues for us to deeply understand the pathogenesis of lung cancer and find new therapeutic targets. They also provide a new nanomedicine delivery strategy for the treatment of lung cancer.

Abbreviations

ATG: Autophagy-related protein; BECN1: Beclin-1; Cu: Cucurbitacin; DMEM: Dulbecco's modified Eagle medium; EPR: Enhanced permeability and retention; ERK: Extracellular signal-regulated kinase; GAPDH: Glyceraldehyde-3-phosphate dehydrogenase; JAK2: Janus kinase 2; LC3: Microtubule-associated protein 1A/1B-light chain 3; LDH: Lactate dehydrogenase; MAPK: Mitogen-activated protein kinase; mTOR: Mammalian target of rapamycin; MTT: 3-(4,5-Dimethylthiazol-2-yl)-2,5-diphenyltetra zolium bromide; PI3K: Phosphoinositide 3-kinase; ROS: Reactive oxygen species; RPMI-1640: Roswell Park Memorial Institute-1640; RT-PCR: Reverse transcription polymerase chain reaction; SLC7A11: Solute carrier family 7 member 11; STAT3: Signal transducer and activator of transcription 3; TPP: Tripolyphosphate; VEGF: Vascular endothelial growth factor; WB: Western blot.

Declaration of Conflicting Interests

The authors declared no potential conflicts of interest with respect to the research, authorship, and/or publication of this article.

Ethical Approval

This study was approved by the ethics committee of Beichen District Traditional Chinese Medicine Hospital, affiliated to Tianjin University of Traditional Chinese Medicine.

Funding

The authors received no financial support for the research, authorship, and/or publication of this article.

ORCID iD

Tao Zhang https://orcid.org/0000-0002-9748-6056

Informed Consent

Not applicable.

References

Basha, S. Z., Mohamed, G. A., Abdel-Naim, A. B., Hasan, A., & Abdel-Lateff, A. (2021). Cucurbitacin E glucoside from *Citrullus colocynthis* inhibits testosterone-induced benign prostatic hyperplasia in mice. *Drug and Chemical Toxicology*, *44*(5), 533–543. https://doi.org/10.1080/01480545.2019.1635149

Brouwer, I. J., Out-Luiting, J. J., Vermeer, M. H., & Tensen, C. P. (2020). Cucurbitacin E and I target the JAK/STAT pathway and induce apoptosis in Sezary cells. *Biochemistry and Biophysics Reports*, *24*, Article 100832. https://doi.org/10.1016/j.bbrep.2020.100832

Chandra, D., Molla, M. T. H., Bashar, M. A., Islam, M. S., & Ahsan, M. S. (2023). Chitosan-based nano-sorbents: Synthesis, surface modification, characterisation and application in Cd(II), Co(II). *Scientific Reports*, *13*(1), 6050. https://doi.org/10.1038/s41598-023-32847-3

Chen, X., Li, S., Li, D., Li, M., Su, Z., Lai, X., Zhou, C., Chen, S., Li, S., Yang, X., Su, J., & Zhang, Y. (2020). Ethanol extract of *Brucea javanica* seed inhibit triple-negative breast cancer by restraining autophagy via PI3K/Akt/mTOR pathway. *Frontiers in Pharmacology*, *11*, 606. https://doi.org/10.3389/fphar.2020.00606

Deleyto-Seldas, N., & Efeyan, A. (2021). The mTOR-autophagy axis and the control of metabolism. *Frontiers in Cell and Developmental Biology*, *9*, Article 655731. https://doi.org/10.3389/fcell.2021.655731

Dunn, S., Eberlein, C., Yu, J., Gris-Oliver, A., Ong, S. H., Yelland, U., Cureton, N., Staniszewska, A., McEwen, R., Fox, M., Pilling, J., Hopcroft, P., Coker, E. A., Jaaks, P., Garnett, M. J., Isherwood, B., Serra, V., Davies, B. R., Barry, S. T., & Yusa, K. (2022). AKT-mTORC1 reactivation is the dominant resistance driver for PI3Kβ/AKT inhibitors in PTEN-null breast cancer and can be overcome by combining with Mcl-1 inhibitors. *Oncogene*, *41*(46), 5046–5060. https://doi.org/10.1038/s41388-022-02482-9

Guo, Q.-Q., Wang, S.-S., Zhang, S.-S., Xu, H.-D., Li, X.-M., Guan, Y., Yi, F., Zhou, T.-T., Jiang, B., Bai, N., Ma, M.-T., Wang, Z., Feng, Y.-L., Guo, W.-D., Wu, X., Zhao, G.-F., Fan, G.-J., Zhang, S.-P., Wang, C.-G., & Cao, L. (2020). ATM-CHK2-Beclin 1 axis promotes autophagy to maintain ROS homeostasis under oxidative stress. *The EMBO Journal*, *39*(10), Article e103111. https://doi.org/10.15252/embj.2019103111

He, S., & Tang, S. L. (2020). WNT/beta-catenin signaling in the development of liver cancers. *Biomedicine and Pharmacotherapy*, *132*, Article 110851. https://doi.org/10.1016/j.biopha.2020.110851

Hirata, Y., Nomura, K., Kato, D., Wake, H., Ogawa, W., Hirata, Y., Tachibana, Y., Niikura, T., Uchiyama, K., Hosooka, T., Fukui, T., Oe, K., Kuroda, R., Hara, Y., Adachi, T., & Shibasaki, K. (2022). A Piezo1/KLF15/IL-6 axis mediates immobilization-induced muscle atrophy. *The Journal of Clinical Investigation*, *132*(10), 1–13. https://doi.org/10.1172/JCI154611

Ikeda, S.-I., Kurihara, T., Jiang, X. Y., Miwa, Y., Lee, D., Serizawa, N., Jeong, H., Mori, K., Katada, Y., Kunimi, H., Ozawa, N., Shoda, C., Ibuki, M., Negishi, K., Torii, H., & Tsubota, K. (2022). Scleral PERK and ATF6 as targets of myopic axial elongation of mouse eyes. *Nature Communications*, *13*(1), 5859. https://doi.org/10.1038/s41467-022-33605-1

Kim, J. Y., Kim, M.-J., Lee, J. S., Son, J., Kim, D.-H., Lee, J. S., Jeong, S.-K., Chun, E., & Lee, K.-Y. (2022). Stratifin (SFN) regulates lung cancer progression via nucleating the Vps34-BECN1-TRAF6 complex for autophagy induction. *Clinical and Translational Medicine*, *12*(6), e896. https://doi.org/10.1002/ctm2.896

Kim, M.-J., Min, Y., Jeong, S.-K., Son, J., Kim, J. Y., Lee, J. S., Kim, D.-H., Lee, J. S., Chun, E., & Lee, K.-Y. (2022). USP15 negatively regulates lung cancer progression through the TRAF6-BECN1 signaling axis for autophagy induction. *Cell Death and Disease*, *13*(4), 348. https://doi.org/10.1038/s41419-022-04808-7

Kumari, S., Singh, P., Dash, D., & Singh, R. (2024). Understanding the molecular basis of anti-fibrotic potential of intranasal curcumin and its association with mitochondrial homeostasis in silica-exposed mice. *Mitochondrion*, *78*, Article 101943. https://doi.org/10.1016/j.mito.2024.101943

Kumari, S., Singh, P., & Singh, R. (2024). Repeated silica exposures lead to silicosis severity via PINK1/PARKIN mediated mitochondrial dysfunction in mice model. *Cellular Signalling*, *121*, Article 111272. https://doi.org/10.1016/j.cellsig.2024.111272

Leng, J., Dai, X., Cheng, X., Zhou, H., Wang, D., Zhao, J., Ma, K., Cui, C., Wang, L., & Guo, Z. (2022). Biomimetic cucurbitacin B-polydopamine nanoparticles for synergistic chemo-photothermal therapy of breast cancer. *Frontiers in Bioengineering and Biotechnology*, *10*, Article 841186. https://doi.org/10.3389/fbioe.2022.841186

Li, Y. D., Feng, J., Song, S., Li, H. T., Yang, H. J., Zhou, B., Li, Y., Yue, Z., Lian, H., Liu, L. H., Hu, S. S., & Nie, Y. (2020). gp130 controls cardiomyocyte proliferation and heart regeneration. *Circulation*, *142*(10), 967–982. https://doi.org/10.1161/CIRCULATIONAHA.119.044484

Liao, J., Zhang, S. S., Yang, S. T., Lu, Y., Lu, K., Wu, Y. W., Wu, Q. F., Zhao, N., Dong, Q., Chen, L., & Du, Y. M. (2021). Interleukin-6-mediated-Ca^{2+} handling abnormalities contributes to atrial fibrillation in sterile pericarditis rats. *Frontiers in Immunology*, *12*, Article 758157. https://doi.org/10.3389/fimmu.2021.758157

Lin, X. K., & Farooqi, A. A. (2021). Cucurbitacin mediated regulation of deregulated oncogenic signaling cascades and non-coding RNAs in different cancers: Spotlight on JAK/STAT, Wnt/beta-catenin, mTOR, TRAIL-mediated pathways. *Seminars in Cancer Biology*, *73*, 302–309. https://doi.org/10.1016/j.semcancer.2020.10.012

Liu, J. Q., Xiao, Q., Xiao, J. N., Niu, C. X., Li, Y. Y., Zhang, X. J., Zhou, Z. W., Shu, G., & Yin, G. (2022). Wnt/beta-catenin signalling: Function, biological mechanisms, and therapeutic opportunities. *Signal Transduction and Targeted Therapy*, *7*(1), 3. https://doi.org/10.1038/s41392-021-00762-6

Nooreldeen, R., & Bach, H. (2021). Current and future development in lung cancer diagnosis. *International Journal of Molecular Sciences*, *22*(16), Article 8661. https://doi.org/10.3390/ijms22168661

Ouyang, S., Li, H., Lou, L., Huang, Q., Zhang, Z., Mo, J., Li, M., Lu, J., Zhu, K., Chu, Y., Ding, W., Zhu, J., Lin, Z., Zhong, L., Wang, J., Yue, P., Turkson, J., Liu, P., Wang, Y., & Zhang, X. (2022). Inhibition of STAT3-ferroptosis negative regulatory axis suppresses tumor growth and alleviates chemoresistance in gastric cancer. *Redox Biology*, *52*, Article 102317. https://doi.org/10.1016/j.redox.2022.102317

Singh, P., Kumari, S., Chakravortty, H., Pandey, A., Dash, D., & Singh, R. (2025). *In vivo, in vitro*, and *in silico* approaches in the detailed study of di-butyl phthalate (DBP), a plasticizer-induced lung fibrosis via Nrf-2/Keap-1/HO-1 pathway and its regulation. *Bioorganic Chemistry*, *154*, Article 107970. https://doi.org/10.1016/j.bioorg.2024.107970

Son, J., Kim, M.-J., Lee, J. S., Kim, J. Y., Chun, E., & Lee, K.-Y. (2021). Hepatitis B virus X protein promotes liver cancer progression through autophagy induction in response to TLR4 stimulation. *Immune Network*, *21*(5), e37. https://doi.org/10.4110/in.2021.21.e37

Sun, P., Jin, J., Wang, L. X., Wang, J. J., Zhou, H. C., Zhang, Q., & Xu, X. G. (2021). Porcine epidemic diarrhea virus infections induce autophagy in Vero cells via ROS-dependent endoplasmic reticulum stress through PERK and IRE1 pathways. *Veterinary Microbiology*, *253*, Article 108959. https://doi.org/10.1016/j.vetmic.2020.108959

Torres-Moreno, H., Marcotullio, M. C., Velazquez, C., Arenas-Luna, V. M., Hernández-Gutiérrez, S., & Robles-Zepeda, R. E. (2020). Cucurbitacin IIb from *Ibervillea sonorae* induces apoptosis and cell cycle arrest via STAT3 inhibition. *Anti-Cancer Agents in Medicinal Chemistry*, *20*(10), 1188–1196. https://doi.org/10.2174/1871520620666200415101701

Üremiş, N., Üremiş, M. M., Çiğremiş, Y., Tosun, E., Baysar, A., & Türköz, Y. (2022). Cucurbitacin I exhibits anticancer efficacy through induction of apoptosis and modulation of JAK/STAT3, MAPK/ERK, and AKT/mTOR signaling pathways in HepG2 cell line. *Journal of Food Biochemistry*, *46*(10), Article e14333. https://doi.org/10.1111/jfbc.14333

Wu, Z., Stangl, S., Hernandez-Schnelzer, A., Wang, F., Hasanzadeh Kafshgari, M., Bashiri Dezfouli, A., & Multhoff, G. (2023). Functionalized hybrid iron oxide-gold nanoparticles targeting membrane Hsp70 radiosensitize triple-negative breast cancer cells by ROS-mediated apoptosis. *Cancers*, *15*(4), Article 1167. https://doi.org/10.3390/cancers15041167

Yang, P., Liu, W., Fu, R., Ding, G.-B., Amin, S., & Li, Z. Y. (2020). Cucurbitacin E chemosensitizes colorectal cancer cells via mitigating TFAP4/Wnt/beta-catenin signaling. *Journal of Agricultural and Food Chemistry*, *68*(48), 14148–14160. https://doi.org/10.1021/acs.jafc.0c05551

Yuan, B., Clowers, M. J., Velasco, W. V., Peng, S. P., Peng, Q., Shi, Y. W., Ramos-Castaneda, M., Zarghooni, M., Yang, S. Y., Babcock, R. L., Chang, S. H., Heymach, J. V., Zhang, J. J., Ostrin, E. J., Watowich, S. S., Kadara, H., & Moghaddam, S. J. (2022). Targeting IL-1? As an immunopreventive and therapeutic modality for K-ras-mutant lung cancer. *JCI Insight*, *7*(11), Article e157788. https://doi.org/10.1172/jci.insight.157788

Yuan, R. Y. K., Zhao, W. T., Wang, Q.-Q., He, J., Han, S., Gao, H. W., Feng, Y. L., & Yang, S. L. (2021). Cucurbitacin B inhibits non-small cell lung cancer *in vivo* and *in vitro* by triggering TLR4/NLRP3/GSDMD-dependent pyroptosis. *Pharmacological Research*, *170*, Article 105748. https://doi.org/10.1016/j.phrs.2021.105748

Zanders, L., Kny, M., Hahn, A., Schmidt, S., Wundersitz, S., Todiras, M., Lahmann, I., Bandyopadhyay, A., Wollersheim, T., Kaderali, L., Luft, F. C., Birchmeier, C., Weber-Carstens, S., & Fielitz, J. (2022). Sepsis induces interleukin 6, gp130/JAK2/STAT3, and muscle wasting. *Journal of Cachexia, Sarcopenia and Muscle*, *13*(1), 713–727. https://doi.org/10.1002/jcsm.12867

Zhang, J. X., Yuan, L., Wang, S. J., Liu, J., Bi, H. Q., Chen, G. J., Li, J. J., & Chen, L. L. (2020). Germacrone protects against oxygen-glucose deprivation/reperfusion injury by inhibiting autophagy processes in PC12 cells. *BMC Complementary Medicine and Therapies*, *20*(1), 77. https://doi.org/10.1186/s12906-020-2865-1

Zhang, Z. Z., Richmond, A., & Yan, C. (2022). Immunomodulatory properties of PI3K/AKT/mTOR and MAPK/MEK/ERK inhibition augment response to immune checkpoint blockade in melanoma and triple-negative breast cancer. *International Journal of Molecular Sciences*, *23*(13), Article 7353. https://doi.org/10.3390/ijms23137353

Zheng, S. H., Shi, B. W., Li, X., Yuan, H., & Feng, Y. L. (2022). Cucurbitacin E reduces the cognitive dysfunction induced by sevoflurane in rats by regulating NF-kappa B pathway. *Acta Biochimica Polonica*, *69*(2), 387–391. https://doi.org/10.18388/abp.2020_5817

Zhou, L., Wang, S. S., Cao, L. N., Ren, X. M., Li, Y. H., Shao, J. H., & Xu, L. C. (2021). Lead acetate induces apoptosis in Leydig cells by activating PPAR gamma/caspase-3/PARP pathway. *International Journal of Environmental Health Research*, *31*(1), 34–44. https://doi.org/10.1080/09603123.2019.1625034

Zhou, Q., Cui, F., Lei, C., Ma, S., Huang, J., Wang, X., Qian, H., Zhang, D., & Yang, Y. (2021). ATG7-mediated autophagy involves in miR-138-5p regulated self-renewal and invasion of lung cancer stem-like cells derived from A549 cells. *Anti-cancer Drugs*, *32*(4), 376–385. https://doi.org/10.1097/CAD.0000000000000979